Bulletin of Geophysics and Oceanography Vol. 66, n. 4, pp. 447-458; December 2025
DOI 10.4430/bgo00498

Regional interpretation of gravity data using the Riesz transform method: the case of the Tanezrouft region, southern Algeria

L. Harrouchi[1,2], M.-C. Berguig[2], R. Boutrika[3] and M.S. Beleksier[4]

[1] *Sahara Geology Laboratory, Kasdi Merbah University, Ouargla, Algeria*
[2] *Geophysics Laboratory, FSTGAT/USTHB, Bab Ezzouar, Algeria*
[3] *Metallogeny and Magmatism Laboratory, FSTGAT/USTHB, Bab Ezzouar, Algeria*
[4] *Laboratory of Underground Reservoirs, Kasdi Merbah University, Ouargla, Algeria*

(Received: 15 May 2024; accepted: 7 July 2025; published online: 28 November 2025)

ABSTRACT In this study, we interpreted regional gravity data from the Tanezrouft region in southern Algeria using the Riesz transform (RT) method, in combination with Energy Spectrum (ES) analysis. The RT method was applied to both synthetic and real gravity data to locate and estimate the depths of gravity sources in the study area. Three distinct depth ranges were identified based on their spectral characteristics: short-wavelength anomalies (depths < 2.65 km), medium-wavelength anomalies (2.65 km < depths < 7.25 km), and long-wavelength anomalies (depths > 7.25 km). These depth classes were confirmed by applying three dimensional Euler deconvolution to the RT results using specific parameters. The depths derived from the Euler solutions closely matched the ES inversion results. Furthermore, the Upward Continuation filter applied to the RT results at 20 km revealed two significant negative anomalies. The first one, including the development of various fault systems, is located in the west and is attributed to the collision of the Hoggar Mountains with the West African Craton. The second, instead, is situated in the east and is caused by a NE-oriented oblique fault system associated with a rifting zone that diagonally traverses the study area.

Key words: regional interpretation, gravity data, Tanezrouft region, Riesz transform, 3D Euler deconvolution, Upward Continuation.

1. Introduction

Despite the available geophysical studies of the area of the Tanezrouft region, including magnetic, gamma-ray spectrometric (Aeroservice, 1975), ground-based gravity (Bourmatte, 1977), and magnetotelluric surveys (Bouzid *et al*., 2008), the structural features of this area remained poorly understood.

This paper is dedicated to the estimate of the geometrical parameters of the gravimetric sources of the Tanezrouft region, in southern Algeria. In this optic, we applied the Riesz transform (RT) and Energy Spectrum (ES) inversion methods both on synthetic and real gravity data of the study area. The use of the RT method is motivated by its robustness and effectiveness in delineating the geometric shapes and boundaries of geological structures (Hidalgo-Gato and Barbosa, 2015).

Harrouchi *et al*. (2020) validated the effectiveness of the RT method using the concepts of monogenic signal with the Cauchy Riemann conditions. They obtained a new expression for the Riesz Analytic Signal Amplitude (*RASA*) and the Riesz Local Phase (RLP), respectively. The tests on

a synthetic model showed that RASA and RLP performed better in delineating geological contacts that were not visible in the original data. Another important advantage of the RT method is that it is less sensitive to noise (Harrouchi *et al.*, 2020).

The three dimensional (3D) Euler deconvolution (ED) technique produces automatic depth solutions from gravity data (Reid *et al*., 2003), according to the Structural Index (SI) parameter, and moving window size (WS) cell, used in the calculation. The ED analytical method is based on a mathematical development represented by the Euler homogeneity equation (Thompson, 1982). For gravimetric sources, the 3D ED technique has been applied to the RT method, using an SI = 0, an 11×11 (grid points) moving WS cell, and a 15% tolerance.

To separate the different gravimetric anomaly sources of the Tanezrouft region, we applied several heights: 2, 5, 10, and 20 km of Upward Continuation (UpC), respectively. This method enabled us to confirm some geologic hypothesis.

In this study, we will use the Oasis Montaj software (Geosoft, 2007) to plot the transformed gravity maps of the synthetic model and of our study area.

2. Methodology

The two dimensional (2D) monogenic signal with three components can be expressed in the form (Felsberg and Sommer, 2001, 2004; Hidalgo-Gato and Barbosa, 2015; Li and Pilkington, 2016; Harrouchi *et al*., 2020):

$$F_M = R_x(F)\vec{e}_x + R_y(F)\vec{e}_y + F\vec{e}_z \tag{1}$$

where ($\vec{e}_x$, $\vec{e}_y$, $\vec{e}_z$) are orthogonal bases and R_x and R_y are components *x* and *y* of the first-order RT of *F* (real signal) defined by Felsberg and Sommer (2001) as follows:

$$R_x(F) = \frac{x}{2\pi(x^2+y^2)^{\frac{3}{2}}} * F \tag{2a}$$

$$R_y(F) = \frac{y}{2\pi(x^2+y^2)^{\frac{3}{2}}} * F \tag{2b}$$

where the asterisk (*) represents convolution.

Using this 3D vector representation of the monogenic signal (Fig. 1), we can define (Felsberg and Sommer, 2001; Hidalgo-Gato and Barbosa, 2015; Harrouchi *et al.,* 2020):

$$RASA = \sqrt{(R_xF)^2 + \left(R_yF\right)^2 + F^2} \tag{3}$$

and magnitude RT (*MRT*) given by:

$$MRT = \sqrt{(R_xF)^2 + \left(R_yF\right)^2}. \tag{4}$$

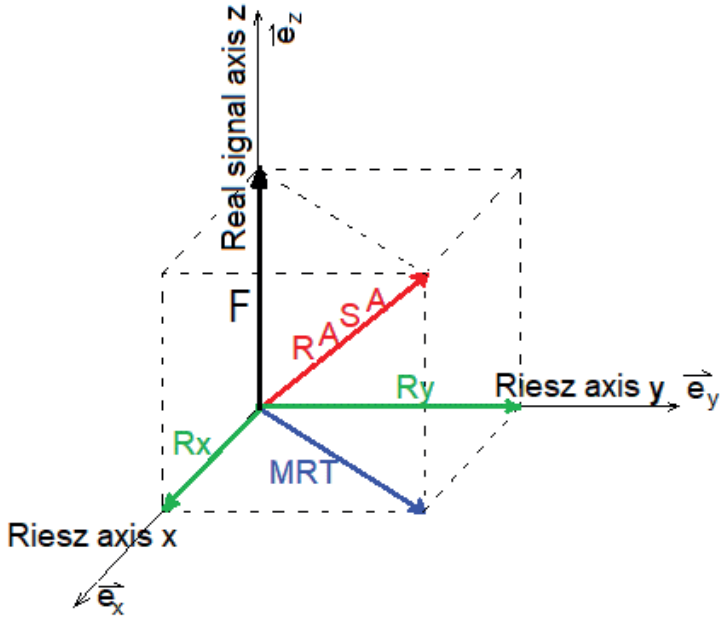

Fig. 1 - Schematic representation of the monogenic signal in 3D Euclidean space. Component *F* is the real signal and components R_x and R_y are the and components of the first-order RT of the real signal. The Riesz analytic signal amplitude and magnitude of components *x* and *y* of the first-order RT are *RASA* and *MRT*, respectively.

The detailed numerical development of the RT method offers a robust foundation for interpreting potential field data as reported in Harrouchi *et al.* (2020).

3. Synthetic gravity data

The RT method has been applied to a synthetic gravity model of prisms A, B, and C, respectively (Fig. 2a). The contact model presumably represents an extreme and simplified model of real geological structures (Beiki and Pedersen, 2010). The shapes [dimensions (length×height×width) in kilometres] of prism A, B, and C are 40×4×15, 15×4×50, and 30×4×30, respectively (Fig. 2a and Table 1), with a density contrast of 0.2 g/cm^3. The depths of the prisms (A, B, and C) are 3, 1, and 7 km, respectively (Table 1). The gravity data anomaly is calculated on a regular grid with a spacing of 1 km (Fig. 2b).

Table 1 - Physical parameters of the synthetic model for prisms A, B, and C.

Physical parameters	Prism A	Prism B	Prism C
Horizontal position x (km)	70	15	70
Horizontal position y (km)	80	50	30
Depth Z (km)	3	1	7
Width (km)	15	50	30
Length (km)	40	15	30
Height (km)	4	4	4
Density contrast (g/cm^3)	0.2	0.2	0.2
Strike (degree)	90°	90°	45°
Slope (degree)	90°	90°	90°

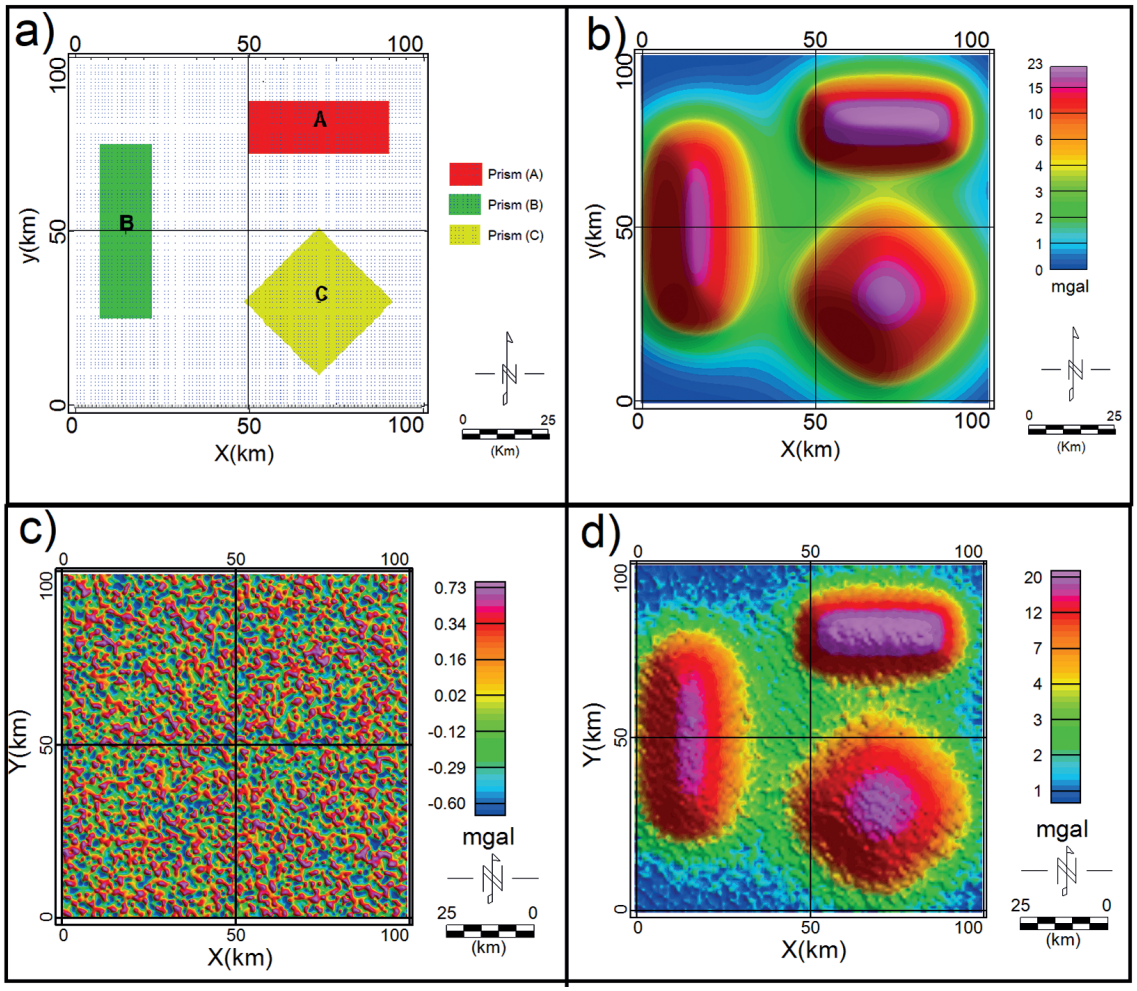

Fig. 2 - a) Plan view of the gravimetric model consisting in three vertical prisms; b) the model gravimetric response; c) Gaussian noise with a standard deviation of approximately 0.8 mGal; d) gravimetric response noised by Fig. 2c.

The gravity data anomaly was corrupted with pseudorandom zero-mean Gaussian noise with a standard deviation of 0.8 mGal (Fig. 2c). The calculation has been applied on the gravity response of the synthetic model (Fig. 2d).

The RT method has been applied to a synthetic gravity model. We determined Figs. 3a and 3b of R_x and R_y by applying Eqs. (2a) and (2b), respectively.

To obtain the horizontal position of the bodies (Fig. 3c), we used Eq. (3), which enabled us to obtain the *RASA* (Fig. 3c). Fig. 3d shows the *MRT* of the *x* and *y* components of the first-order RT obtained with Eq. (4) and also shows the limits of the three prisms.

The ES analysis enabled the identification of three cut-off frequencies related to the change of spectrum slope (Fig. 3e and Table 2). The first one is characterised by a short wavelength, depth (Z) < 2.17 km, the second one is characterised by a medium wavelength, 2.17 km < Z < 6.71 km, and the last one is characterised by a long wavelength, 6.71 km < Z.

To situate these three previous classes horizontally, we used 3D ED (Reid *et al.*, 1990). In this study, the ED method was applied to a synthetic gravity model (Fig. 3f) using SI = 0 (gravity

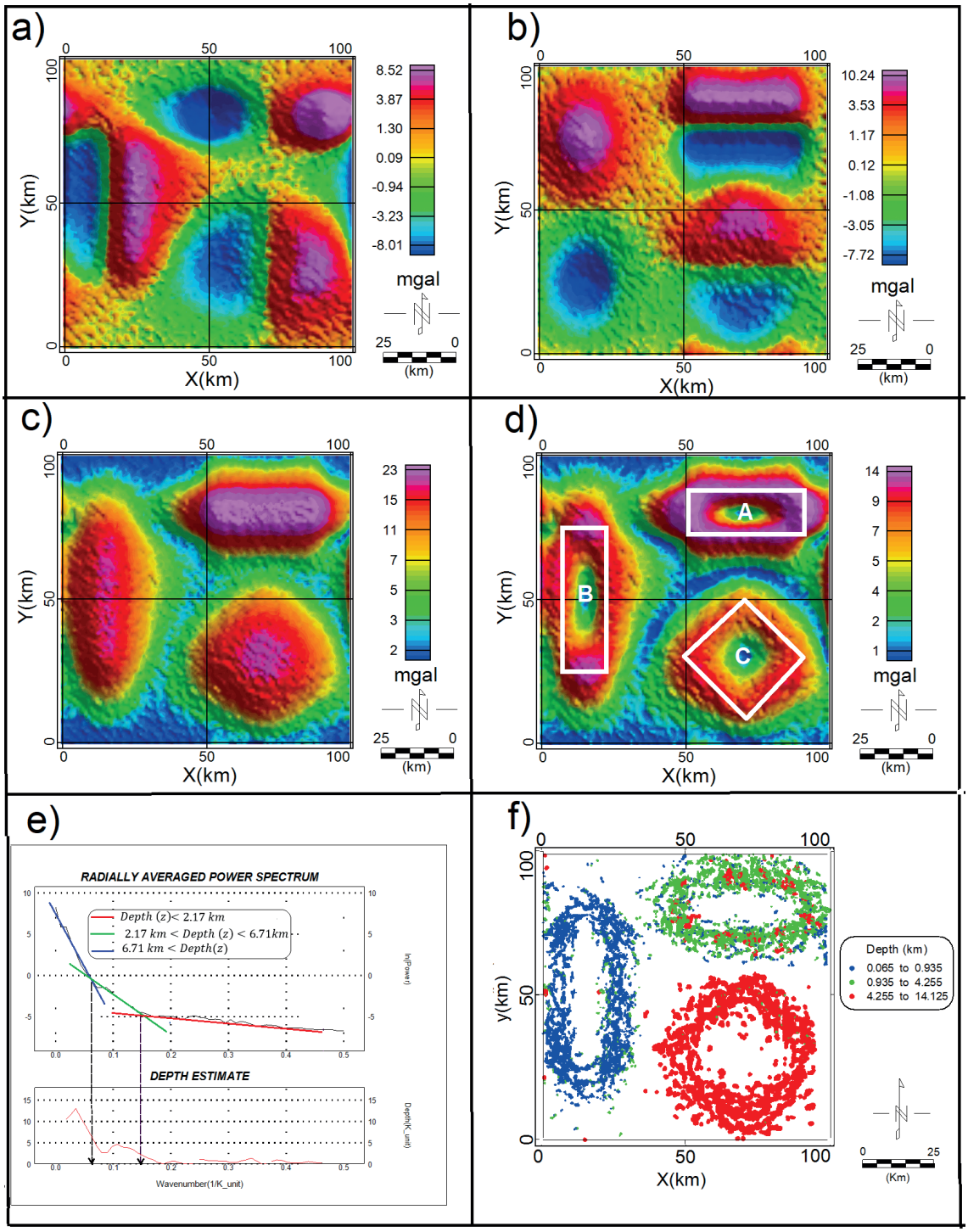

Fig. 3 - Solution of the RT method; a) Riesz axis *x* (R_x) of data from Fig. 2d, obtained from Eq. (2a); b) Riesz axis *y* (R_y) of data from Fig. 2d, obtained from Eq. (2b); c) *RASA* of data from Fig. 2d, obtained from Eq. (3); d) *MRT* of data from Fig. 2d, obtained from Eq. (4); the solid white line represents the shape of the synthetic model; e) solution of the ES method of data from Fig. 3d; f) solution of ED of data from Fig. 3d, using SI = 0, WS = 11×11 (grid points), and a 15% tolerance.

Table 2 - Analysis of the ES of the synthetic gravity model.

Classification	Depth (Z) km
Short wavelength	Z < 2.17
Medium wavelength	2.17 < Z < 6.71
Long wavelength	6.71 < Z

sources), WS = 11×11 (grid points), and a 15% tolerance. The ES and ED methods provide an estimate close to the data initially proposed for the synthetic model (see Figs. 3e and 3f). We can, therefore, confidently apply the two previous methods to real gravity data from the Tanezrouft region.

4. Real data of the study area

Fig. 4a represents the Bouguer gravity anomaly of the study area, obtained from the gravity survey carried out in the Tanezrouft region [West African Craton (WAC), Tassendjanet (Tas),

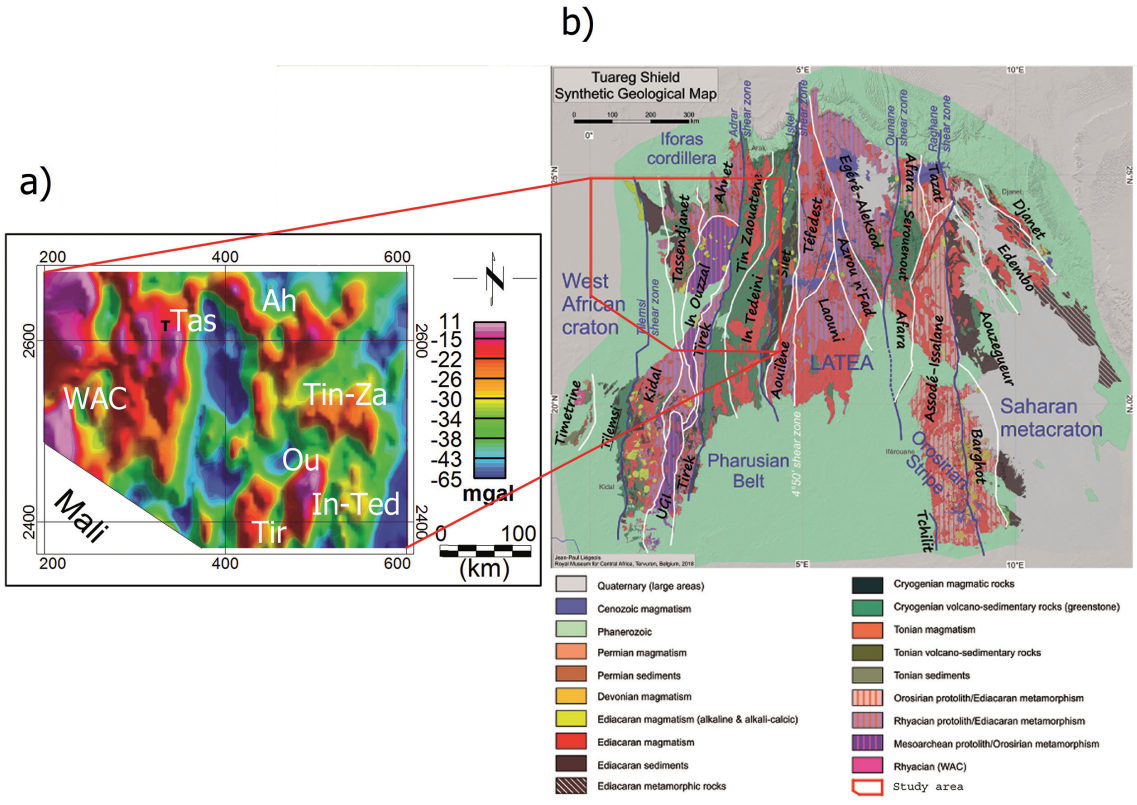

Fig. 4 - a) Bouguer anomaly maps of the study area, showing positive and negative anomalies, with variable dimensions and amplitudes and values ranging between -65 mGal and 11 mGal; b) square plotted in the synthetic geological map of the Tuareg Shield (after Liégeois, 2019) representing the localisation of the study area (WAC = West African Craton; Tas = Tassendjanet, Ou = In Ouzzal; Ah = Ahnet; Tir = Tirek; Ti-Za = Tin-Zaoautene; In-Ted = In Tedeini).

In Ouzzal (Ou), Ahnet (Ah), Tirek (Tir), Tin-Zaouatene (Ti-Za), In Tedeini (In-Ted) terranes], southern Algeria (Fig. 4b) between 1974 and 1975 (Bourmatte, 1977). The EW-oriented profiles are practically perpendicular to the main sub-meridian directions. For mapping local geological structures, the survey employed profiles with an average spacing of 18 km and measurement points spaced at 3-kilometre intervals (Fig. 4a), establishing this as a regional-scale interpretation. The complete technical specifications of the Tanezrouft gravity survey are presented in Table 3. The observed Bouguer anomaly comprises two components: 1) a regional anomaly reflecting deep crustal structures and 2) a residual anomaly representing shallower geological features.

Table 3 - The technical data of the gravity survey of the study area (Bourmatte, 1977).

Materials and techniques used	**Characteristics**
Gravimeters	Three Worden gravimeters type Master no. 600, 660, and 683.
Reduction of measurement	The theoretical values of *g* were calculated using the 1931 international gravity formula; the *g* values are reported in the classic Potsdam System (981274.0 mGal).
Stations used	Beacon 250 levelling posts no. 83 (*g* = 976836.9 mGal); approximate occupancy of the 1987 base of the Lagrula network.
Altimetry	Determination of altitudes using barometric levelling, and using the IGN levelling landmark along the Adrar Gao road.
Planimetry	The position of the stations was determined by compass survey and car speedometer. The starting point of the surveys is the nautical 250; a topographic canvas was realised by the Sonatrach company towards the 0° meridian (Bourmatte, 1977).

In this present work, we have calculated the regional anomaly by means of a first-degree polynomial surface (Fig. 5a). The map of residual gravity anomalies (Fig. 5b) has been obtained by subtracting this polynomial from the Bouguer anomaly data. The coefficients of the polynomial are shown in Table 4. We verified that the sum of the residual gravity anomalies is close to zero as shown in the histogram of Fig. 5c. This means that the residual gravity anomalies have a zero mathematical expectation, which means that polynomial *P(x, y)* is adequate to the gravity data in the study area. Thus, we applied the ES (Fig. 5d) to the Bouguer anomalies (Fig. 5b). This spectrum provides a general idea on the separation of the short and long wavelengths of origin of the gravimetric sources. The analysis of the ES (Fig. 5d), enables the identification of three cut-off frequencies associated with the change in slope of the spectrum. It is, therefore, possible to classify the gravity anomalies in our study area into three distinct categories (Table 5).

The first category includes short wavelength anomalies (Z < 2.65 km), the second is composed of medium wavelength anomalies (2.65 km < Z < 7.25 km), and the last regroups the long wavelengths (Z > 7.25 km).

Table 4 - The polynomial coefficients: $P(x,y) = a+bx+cy$.

a	13.7883 mGal
b	-0.07122 mGal/km
c	-0.001015 mGal/km

Table 5 - Analysis of the Tanezrouft gravity data ES.

Classification	Depth (Z) km
Short wavelength	Z < 2.65
Medium wavelength	2.65 < Z < 7.25
Long wavelength	7.25 < Z

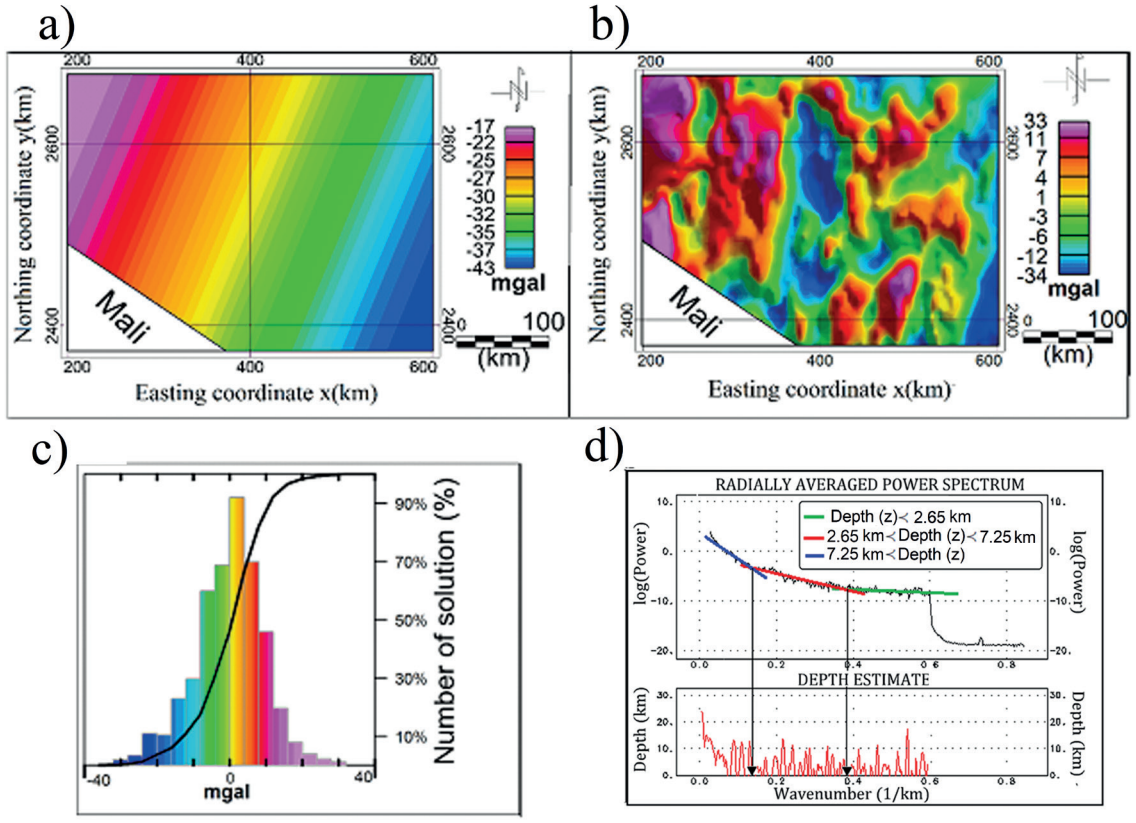

Fig. 5 - a) First degree polynomial surface map; b) residual map of the gravity anomalies [the Cartesian coordinates (*x* and *y*) are given in UTM-zone 31]; c) histogram of the values of the gravity data in Fig. 5b (the sum of the residual gravity anomalies is close to zero); d) solution of the ES method of data from Fig. 4a.

5. Results and discussion

Fig. 6a shows the R_x of the gravimetric residual map, obtained by applying Eq. (2a), highlighting lithological, structural contacts, and tectonic faults which are perpendicular to the *x*-axis. This figure reveals faults oriented in the N-S direction. Conversely, R_y (Fig. 6b) reveals E-W-trending contacts and faults. Figs. 6c and 6d represent the *RASA* and *MRT*, respectively, showing positive and negative anomalies oriented N-S, NE-SW, and NW-SE, in line with the geology of the study area. In the eastern part, the western Ouzzalian and eastern Ouzzalian shear zones of the Ou terrane dip, at the least to the base of the crust, and may represent suture zones (Bouzid *et al.*, 2008). In the central part (Figs. 6b, 6c, and 6d), a strong negative anomaly oriented NE-SW likely

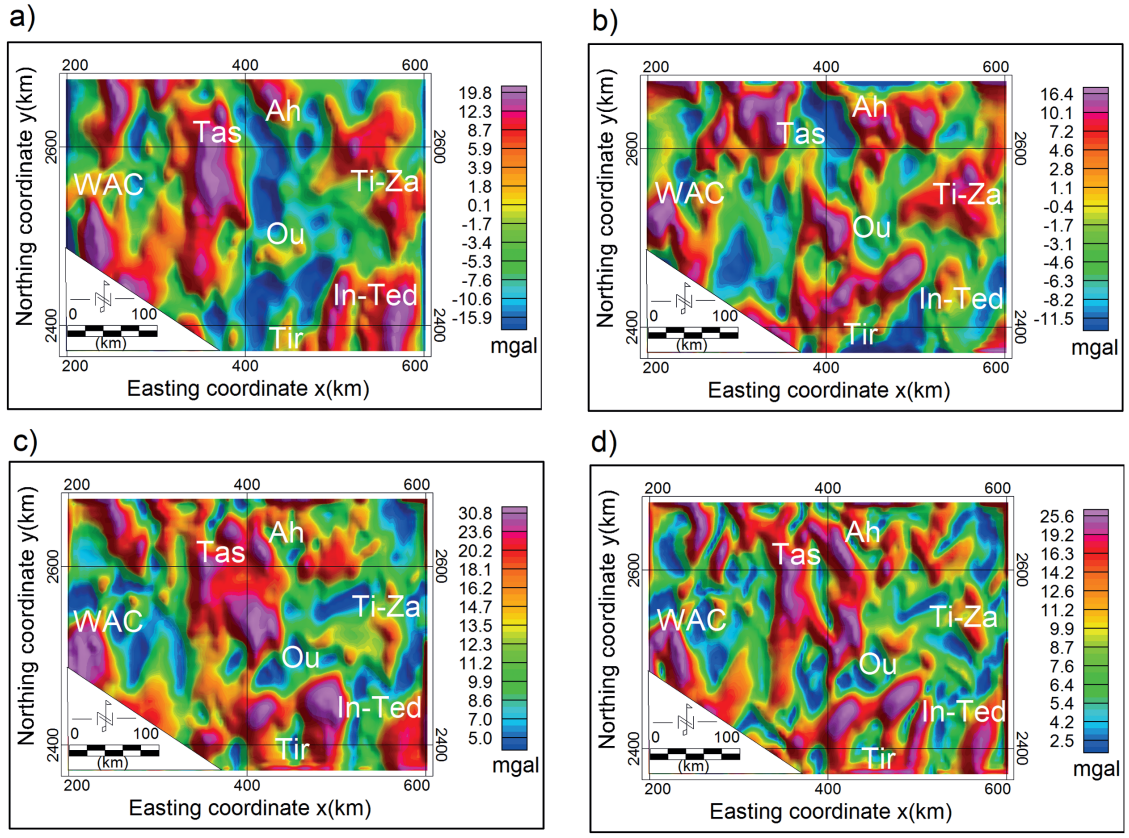

Fig. 6 - Solution from the RT method of the Tanezrouft region: a) R_x of data from Fig. 5b, obtained from Eq. (2a); b) R_y of data from Fig. 5b, obtained from Eq. (2b); c) *RASA* of data from Fig. 5b, obtained from Eq. (3); d) *MRT* of data from Fig. 5b, obtained from Eq. (4) (WAC = West African Craton; Tas = Tassendjanet, Ou = In Ouzzal; Ah = Ahnet; Tir = Tirek; Ti-Za = Tin-Zaoautene; In-Ted = In Tedeini).

indicates a subduction zone (Bournas, 2001). To the west, positive anomalies (Fig. 6c and 6d) indicate the suture of the WAC.

Fig. 7 illustrates the 3D Euler solutions for the study area, showing a perfect agreement between the positions of the Euler solutions and both short- and long-wavelength anomalies

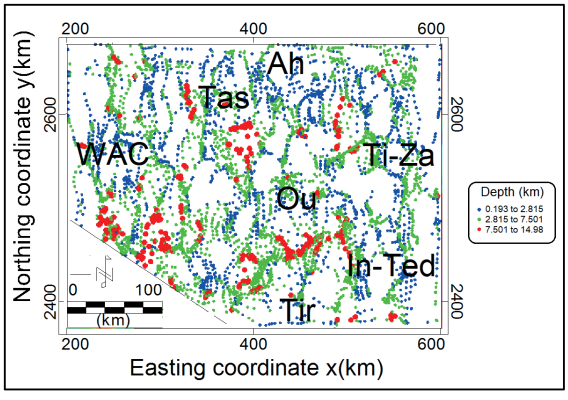

Fig. 7 - Solution of ED of data from Fig. 6c, using SI = 0, WS = 11×11 (grid points) and a 15% tolerance (WAC = West African Craton; Tas = Tassendjanet, Ou = In Ouzzal; Ah = Ahnet; Tir = Tirek; Ti-Za = Tin-Zaoautene; In-Ted = In Tedeini).

associated with various tectonic faults and lithological formations. In this study, the disturbance structure (contact) has been considered using the corresponding Euler parameters: SI = 0, WS = 11×11 (grid points), and a 15% tolerance. The lithological contact between the Ou terrane and the Pharusian trough coincides with the medium-depth solutions (6 km). The western boundary of the Ou with the Tas terrane around the deep solutions (more than 7 km) is likely a subduction zone (Bournas, 2001; Harrouchi *et al.*, 2016). The solutions to the NE of the Ou terrane are bounded by the Ah terrane.

In order to highlight the continuity of the geological structures at depth and to separate various frequency components, which are often associated with noise, we applied the UpC method. This method is known for its stability in processing geophysical data, by effectively separating different frequency bands (Blakely, 1995; Cooper, 2004; Benhadj Tahar and Berguig, 2024). Accordingly, UpC filters were applied to the RASA data as a function of the distance from the continuations. The UpC filters were applied at different heights: at 2 km (Fig. 8a), the gravity anomalies remained but with smoother curves and decreased amplitudes; at 5 km (Fig. 8b), some short-wavelength anomalies disappeared, especially in the eastern and western parts of the study area; at 10 km (Fig. 8c), only long-wavelength anomalies linked to deep sources persisted; and at 20 km (Fig. 8d), anomalies from deep sources were clearly separated and distinguished by

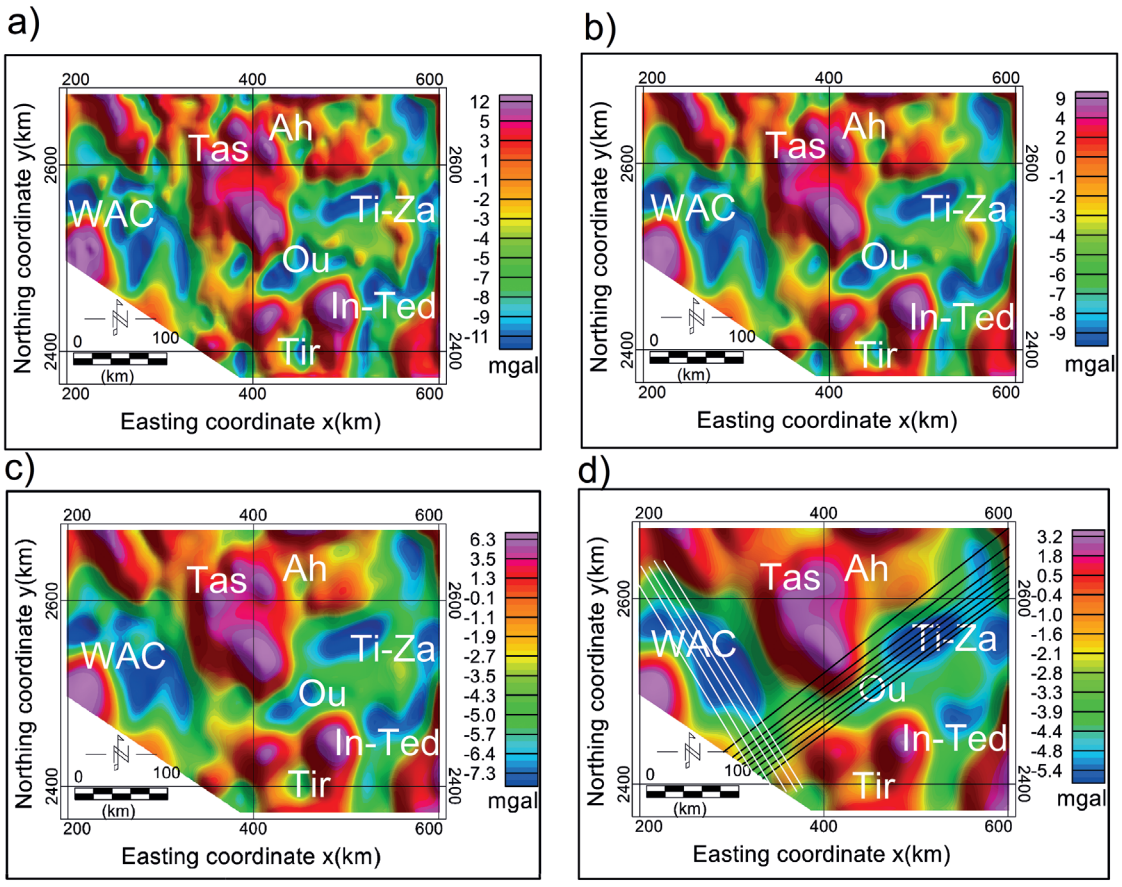

Fig. 8 - UpC maps of *RASA* data; a) at 2 km; b) at 5 km; c) at 10 km; d) at 20 km (WAC = West African Craton; Tas = Tassendjanet, Ou = In Ouzzal; Ah = Ahnet; Tir = Tirek; Ti-Za = Tin-Zaoautene; In-Ted = In Tedeini). The solid white lines represent the collision of the Hoggar with the WAC while solid black lines represent the rifting zone.

their amplitudes. At this altitude, the large groups of anomalies linked to deep sources are well separated and clearly differentiated by their amplitudes. To the west of the study area, the UpC filter (Fig. 8d) highlighted a large negative gravity anomaly caused by the collision of the Hoggar with the WAC during the Pan-African event (Black *et al.*, 1979). The mechanism of this collision has led to the development of several fault systems oriented N-S, NE-SW, and NW-SE (see Fig. 6d).

The NE-trending oblique fault system revealed in the east of the study area is thought to be associated with a rifting zone, crossing the region diagonally over a distance of several tens of kilometres. This expanse is thought to be responsible for the formation of the graben and complex of basaltic formations aligned in a NE direction (Bournas 2001).

6. Conclusions

The application of the developed approach, utilising the RT method, ES analysis, and 3D ED to the gravity data of the Tanezrouft region in southern Algeria, has effectively demonstrated its utility. The RT method played a pivotal role in enhancing geological features, particularly in the presence of noise, thereby improving our ability to locate and estimate the depths of subsurface structures. Further refinement was achieved through ES analysis, which identified three distinct depth ranges for the gravity sources, corresponding to short, medium, and long wavelengths.

The application of 3D ED to the RT-processed regional gravity data yielded depth estimations that closely aligned with the results from the ES analysis, confirming the presence of distinct geological structures at varying depths. This integrated approach has significantly contributed to elucidating the complex geological setting of the Tanezrouft region.

The insights derived from this study hold important implications for geological mapping and resource exploration in similar regions. By unveiling previously obscured geological features and their depth distribution, this methodology opens new insights for exploration and research. Future studies can capitalise on this approach, which extends its application to other regions with comparable geological characteristics, to validate its effectiveness and explore its broader applicability within geophysics and resource exploration.

The UpC filter at 20 km from the *RASA* data revealed two major negative anomalies: 1) the first, located in the western part of our study area, was attributed to the collision of the Hoggar with the WAC, and 2) the second, situated in the eastern part of our study area, was associated with a system of NE-trending faults and a rifting zone crossing the study area diagonally.

Acknowledgments. The authors express their gratitude to A. Bourmatte from USTHB University for providing the gravimetric data presented in Fig. 4a. Sincere thanks are extended to Kh. Ouzegane from USTHB University for her constructive comments on the manuscript. Special appreciation goes to the editor of the BGO journal for his kind cooperation and assistance.

REFERENCES

Aeroservice; 1975: *Aero-magneto-spectrometric survey of Algeria*. Final report, 3 vols., Houston (TX) - Philadelphia (PA), USA.

Beiki M. and Pedersen L.B.; 2010: *Window constrained inversion of gravity gradient tensor data using dike and contact models*. Geophys., 76, 159-172.

Benhadj Tahar Y. and Berguig M.C.; 2024: *Stable iterative downward continuation of potential field based on Runge-Kutta method.* J. Appl. Geophys., 220, doi: 10.1016/j.jappgeo.2023.105278.

Black R., Caby R., Moussine-Pouchkine A., Bayer A., Bertrand J.M., Boullier A.M., Fabre J. and Lesquer A.; 1979: *Evidence for Late Precambrian plate tectonics in west Africa.* Nature, 278, 223-227.

Blakely R.J.; 1995: *Potential theory in gravity and magnetic applications.* Cambridge University Press, Cambridge, UK, 464 pp., doi: 10.1017/CBO9780511549816.

Bourmatte A.; 1977: *Etude gravimétrique du Tanezrouft*. Thèse d'état, Université des sciences et techniques du Languedoc, Montpellier, France, 143 pp.

Bournas N.; 2001: *Interprétation des données aérogéophysiques acquises au-dessus du Hoggar Oriental.* Thèse Doctorat, Université des Sciences et de la Technologie Houari Boumédiène (USTHB), Alger, Algeria, 250 pp.

Bouzid A., Akacem N., Hamoudi M., Ouzegane K., Abtout A. and Kienast J.R.; 2008: *Modélisation magnétotellurique de la structure géologique profonde de l'unité granulitique de l'In Ouzzal (Hoggar occidental).* C.R. Géosci., 340, 711-722.

Cooper G.; 2004: *The stable downward continuation of potential field data*. Explor. Geophys., 35, 260-265, doi: 10.1071/EG04260.

Felsberg M. and Sommer G.; 2001: *The monogenic signal.* IEEE Trans. Signal Process., 49, 3136-3144, doi: 10.1109/78.969520.

Felsberg M. and Sommer G.; 2004: *The Monogenic scale-space: a unifying approach to phase-based image processing in scale-space.* J. Math. Imaging Vision, 21, 5-26, doi: 10.1023/B:JMIV.0000026554.79537.35.

Harrouchi L., Hamoudi M., Bendaoud A. and Beguiret L.; 2016: *Application 3D Euler deconvolution and improved tilt angle to the aeromagnetic data of In Ouzzal terrane, western Hoggar, Algeria.* Arabian J. Geosci., 9, 508-518, doi: 10.1007/s12517-016-2536-1.

Harrouchi L., Berguig M.-C., Boutrika R., Hamoudi M. and Bendaoud A.; 2020: *Application of Riesz Transform to the aeromagnetic data of the central In Ouzzal terrane and adjacent zone, southern Algeria.* Boll. Geof. Teor. Appl., 61, 487-498, doi: 10.4430/bgta0334.

Hidalgo-Gato M.C. and Barbosa V.C.F.; 2015: *Edge detection of potential-field sources using scale-space monogenic signal: fundamental principles:* Geophys., 80, J27-J36, doi: 10.1190/geo2015-0025.1.

Li X. and Pilkington M.; 2016: *Attributes of the magnetic field, analytic signal and monogenic signal for gravity and magnetic interpretation.* Geophys., 81, J79-J86.

Liégeois J.P.; 2019: *A new synthetic geological map of the tuareg shield: an overview of its global structure and geological evolution.* In: Bendaoud A., Hamimi Z., Hamoudi M., Djemai S. and Zoheir B. (eds), The geology of the Arab world-an overview, Springer Geology, pp. 83-107, doi: 10.1007/978-3-319-96794-3_2.

Oasis Montaj (Geosoft Program); 2007: *Geosoft mapping and application system*, *inc*. Suit 500, Richmond St., west Toronto, ON, Canada.

Reid A.B., Allsop J.M., Granser H., Millett A.J. and Somerton I.W.; 1990: *Magnetic interpretation in three dimensions using Euler deconvolution*. Geophys., 55, 80-91, doi: 10.1190/1.1442774.

Reid A.B., Fitzgerald D. and McInerny P.; 2003: *Euler deconvolution of gravity data.* In: Proc. 73rd SEG Annual International Meeting, Dallas, TX, USA, SEG-2003-0580, doi: 10.13140/2.1.3210.0489.

Thompson D.T.; 1982: *'EULDPH'-a new technique for making computer-assisted depth estimates from magnetic data.* Geophys., 47, 31-37.

Corresponding author: Lakhdar Harrouchi
Sahara Geology Laboratory, Kasdi Merbah University
P.O. Box 511, Ouargla 30000, Algeria
Phone: +213 66 6323288; e-mail: harrouchi.lakhdar@univ-ouargla.dz